Int. J. Heat Mass Transfer. Vol. 27, No. 10, pp. 1855–1864, 1984
Printed in Great Britain

0017–9310/84 $3.00 + 0.00

All-modes heat transfer from a horizontal cylinder situated adjacent to adiabatic, partially enclosing walls

E. M. SPARROW and M. A. ANSARI
Department of Mechanical Engineering, University of Minnesota, Minneapolis, MN 55455, U.S.A.

(*Received* 25 *October* 1983 *and in revised form* 23 *December* 1983)

Abstract—Heat transfer due to all participating modes has been measured for a heated horizontal cylinder in the presence of adjacent adiabatic walls which partially enclose the space in which the cylinder is situated. The three investigated configurations included a vertical wall situated to the side of the cylinder, a horizontal wall beneath the cylinder, and a corner formed by the intersection of the vertical and horizontal walls. The separation distance between the cylinder and the wall(s) was varied parametrically, with the closest spacing between the cylinder periphery and the wall(s) being 1/12 cylinder diameter. In the main body of experiments, the surfaces of both the cylinder and the wall(s) were of high emissivity. In general, the wall–cylinder interactions tended to reduce the cylinder heat transfer, with greater reductions at closer spacings. In the presence of a side wall, the largest measured reductions were about 20%; at spacings of $\frac{1}{4}$ diameter and greater, the reductions were negligible. A bottom wall (without a side wall) caused reductions about 5% greater than those due to the side wall, while the corner–cylinder interactions brought about significantly greater reductions (as much as 40%). Supplementary experiments performed with a low emissivity cylinder demonstrated that radiation effects played a substantial role in the wall-related reductions in cylinder heat transfer.

INTRODUCTION

THERE is extensive concern in the literature with natural convection from a single horizontal cylinder situated in surroundings so expansive as to preclude interaction with walls which partially bound the fluid space in which the cylinder is situated. This no-interaction idealization is often not fulfilled in practice, where pipes or tubes are commonly positioned adjacent to either vertical or horizontal walls or in a corner formed by such walls. The wall–cylinder interactions encompass all three modes of heat transfer, so that it is no longer appropriate to refer to such problems as natural convection problems.

Frequently, the walls are made of low conductivity or, perhaps, of insulating materials. Thus, they can be regarded as adiabatic. Consequently, in the presence of a heated cylinder, the temperature of the parts of the wall(s) that are in near proximity to the cylinder will be higher than that of the ambient fluid. For small clearances, the wall temperature may closely approach that of the heated cylinder.

The wall–cylinder interactions are of a complex or even of a contradictory nature. The walls may block the approach of fluid toward the cylinder and retard, via skin friction, the velocity of the flow induced by the cylinder. These interactions tend to diminish the cylinder heat transfer coefficient. On the other hand, as discussed in the preceding paragraph, the wall temperature will exceed the ambient temperature, so that the walls induce a buoyant flow that is additional to that induced by the heated cylinder. Depending on the geometry of the system, the wall-induced flow tends to enhance the cylinder heat transfer.

Apart from the uncommon situation in which the interacting surfaces are polished metals, radiation is directly competitive with natural convection. The radiative heat transfer may exceed that due to natural convection when the surfaces are of high emissivity and high absorptivity. At very close spacings, direct conduction between the cylinder and the wall may occur. The magnitudes of both the radiation and the direct conduction depend on the relative temperatures of the cylinder and the walls. Although the cylinder temperature may be prescribed, the wall temperature finds its own level. It is the resultant of the complex dynamics of the interacting convection, radiation, and conduction processes, subject to the adiabatic boundary condition.

In view of the foregoing, it is neither appropriate nor, in fact, possible (to a satisfactory level of accuracy) to determine separate heat transfer coefficients for the individual transport processes. Even if, somehow, the individual coefficients could be extracted from experimental data, they could not be readily applied in practice because the temperature distribution on the walls is unknown and could not be readily calculated. From the standpoint of practice, it is most relevant to provide heat transfer information that represents all of the participating transfer processes.

The foregoing discussion provides the background for the experimental research presented in this paper. Consideration is given to the heat transfer characteristics of a heated horizontal cylinder which interacts with three types of wall systems: (a) a vertical wall situated to the side of the cylinder, (b) a horizontal wall situated beneath the cylinder, and (c) a corner formed by the vertical and horizontal walls. For these

NOMENCLATURE

A	cylinder surface area
D	cylinder diameter
g	acceleration of gravity
h	natural convection heat transfer coefficient for a cylinder in expansive surroundings
k	thermal conductivity
L	cylinder length
Nu	natural convection Nusselt number for a cylinder in expansive surroundings
Pr	Prandtl number
Q	all-modes heat transfer rate
Q_{nc}	natural convection heat transfer rate for a cylinder in expansive surroundings
Q_{rad}	radiation heat transfer rate for a cylinder in expansive surroundings
Q^*	heat transfer rate for a cylinder in expansive surroundings, $(Q_{nc}+Q_{rad})$
Ra	Rayleigh number, $[g\beta(T_{cyl}-T_\infty)D^3/\nu^2]Pr$
S_h	distance between periphery of cylinder and side wall
S_v	distance between periphery of cylinder and bottom wall
T_{cyl}	cylinder temperature
T_w	wall temperature
T_∞	ambient air temperature.

Greek symbols

β	coefficient of thermal expansion
ε_{cyl}	emissivity of cylinder surface
ε_w	emissivity of wall(s)
ν	kinematic viscosity.

configurations, an extensive set of cylinder–wall separation distances was investigated, totaling 35 different cases.

The walls were made of insulating materials and were faced with a hydrodynamically smooth plastic film of measured emissivity. The horizontal cylinder was electrically heated and virtually isothermal. It was used with two types of radiation surface properties. In the main body of experiments, the cylinder was covered with the aforementioned smooth plastic film. The film had an emissivity of 0.855, a value representative of painted surfaces. In supplementary experiments, the cylinder presented a highly polished aluminum surface for radiative interchange (measured emissivity of 0.05).

For each wall–cylinder separation distance and each cylinder radiation surface condition, data were collected at five values of the Rayleigh number spanning the order of magnitude range from 2×10^4 to 2×10^5. Additional data runs were made for the cylinder without wall interactions, both for the high emissivity and low emissivity surface finishes. All the experiments were performed in air in a laboratory which possessed ideal characteristics for natural convection work.

The presentation of results was formulated to fulfill three objectives: (a) to provide a direct measure of the effect of wall–cylinder interactions, (b) to be directly applicable to design, and (c) to enable modest extrapolation to surfaces with different radiation properties from those used here.

A search of the literature failed to unearth any prior work that deals directly with the problem investigated here. Two papers were found which are of peripheral relevance but actually deal with a distinctly different problem. In ref. [1], natural convection heat transfer coefficients were measured optically for a horizontal cylinder in the presence of water-cooled walls maintained at the same temperature as the ambient air. This wall boundary condition is highly unlikely from the standpoint of practice, and it eliminates many of the wall–cylinder interactions that are of particular relevance in the present problem. Furthermore, the results of ref. [1] may be flawed because the cylinder was relatively short and its lateral ends were open, thereby inviting fluid inflows at these ends. In ref. [2], water-cooled walls were also used, but here the results may be even more seriously flawed because the wall temperature was different from that of the ambient air (wall temperature lower than ambient). The effect of the difference between the wall and ambient temperatures was not investigated. The results of refs. [1, 2] are actually contradictory, and in both investigations only a modest number of cylinder–wall spacings were used.

THE EXPERIMENTS

Wall–cylinder configurations

The three configurations used here in studying the heat transfer characteristics of a horizontal cylinder in the presence of wall–cylinder interactions are depicted schematically in side views in Figs. 1(a)–(c). Figure 1(a) shows the cylinder situated adjacent to a vertical wall, with the distance of nearest approach of the cylinder to the wall denoted by S_h (h ~ horizontal). The situation where there is a horizontal wall beneath the cylinder is shown in Fig. 1(b), where the vertical distance of nearest approach is denoted by S_v. In the case of the corner, Fig. 1(c), both S_h and S_v have to be independently specified in order to define the location of the cylinder with respect to the walls.

The vertical wall used for both Figs. 1(a) and (c) was made of 5.08 cm thick, closed-pore polystyrene, which

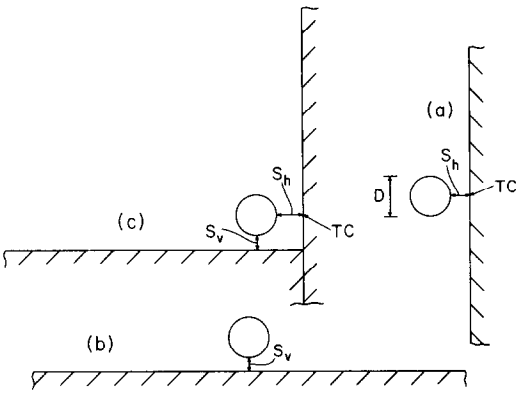

FIG. 1. The investigated wall–cylinder configurations.

was stiffened and held flat by aluminum C-channels mounted on its rear face. A layer of fiberglass (8.9 cm thick) was also affixed to the rear face of the polystyrene in order to achieve the desired thermal resistance. The horizontal walls for Figs. 1(b) and (c) were polystyrene composites, with a total thickness of 15.2 cm and with C-channel stiffeners affixed to the rear face of the uppermost layer of the composite.

To obtain a hydrodynamically smooth surface of known radiation properties, the front faces of the polystyrene walls were covered with white, plasticized, self-adhering contact paper. The emissivity of the contact paper was measured to be 0.855 (the measurement technique will be described shortly).

The vertical wall in Fig. 1 (a) had a height equal to 20 cylinder diameters, and the cylinder was positioned at the mid-height of the wall. The same vertical wall was used in Fig. 1(c), with the same mid-height positioning of the cylinder. For the completion of the corner, a horizontal wall of length equal to 10 cylinder diameters was abutted against the vertical wall as shown in the figure. To guard against the remote possibility of an air leak, the joint was closed with pressure-sensitive tape. In Fig. 1(b), the length of the horizontal wall was 20 diameters, and the cylinder was positioned at the mid-point of the length. For all of the walls, the transverse dimension (i.e. normal to the plane of Fig. 1) was equal to the length of the horizontal cylinder, namely, 20 diameters.

The vertical wall was suspended from a frame fitted with a track which enabled the wall to be moved so as to achieve a continuous variation of the separation distance S_h. The support system for the wall provided the requisite degrees of freedom for the vertical alignment of its front face and for aligning the face so as to be parallel to the horizontal cylinder. A plumb line was used to accomplish the former alignment, while the latter was performed with feeler gauges which also fixed the magnitude of S_h. The horizontal walls of Figs. 1(b) and (c) rested on a table-like frame which provided independent, continuous vertical adjustment at each of the four corners. Horizontal alignment of the walls was accomplished with the aid of a sensitive level, which was also used to align the horizontal cylinder. The spacing S_v was set with feeler gauges.

A thermocouple was installed in the vertical wall at the point of closest approach of the cylinder. The thermocouple was led in from the rear of the wall, and its junction was situated on the rear face of the contact paper. The location of the thermocouple is indicated by the symbol TC in Figs. 1(a) and (c).

Horizontal cylinder

The horizontal cylinder used in the experiments had a diameter D of 3.787 cm and a length L of 76.2 cm, yielding a L/D ratio of about 20. It was made of thick-walled aluminum tubing (0.635 cm thick). The thick wall and high conductivity were chosen to promote temperature uniformity. An additional reason for choosing aluminum (rather than, say, copper) is that it can be polished to a high, enduring luster, which yields a low and timewise constant value of the emissivity suitable for one of the radiative conditions of the present investigation.

Heating was accomplished electrically by a uniformly wound core situated in the bore of the cylinder. The core was made of brass (a good heat conductor). Thermal contact resistance between the core and the cylinder was avoided using copper oxide cement. The core had a hollow bore to allow thermocouple wires from junctions embedded in the cylinder to be led out to the ends.

Seven thermocouples were used to measure the surface temperature of the cylinder. The junctions were actually situated about 0.05 cm from the surface, but it was demonstrated by calculation that the temperature difference between the junction location and the surface was too small to be detected. To minimize possible extraneous conduction along the thermocouple leads, small-gauge, low-conductivity wire was used (0.0127 cm diameter iron–constantan). The thermocouples were calibrated just prior to their installation.

Careful consideration was given to the avoidance of end effects. For one thing, the cylinder was supported at each end through a point contact with a Plexiglas rod, thereby eliminating solid–solid conduction. Furthermore, a baffle made of 2.5 cm thick, resilient, smooth-faced fiberglass was placed in contact with each end of the cylinder. The baffle helped reduce the heat losses from the end faces of the cylinder to the air to a negligible value. Even more important, the baffles served as a curtain which prevented the transverse inflow of air from the ambient toward the cylinder. With these measures, the results obtained here should closely approximate those for an infinitely long cylinder.

In addition to a low emissivity radiative condition represented by the polished aluminum surface, a high emissivity condition was obtained by covering the cylinder with the same white, plasticized, self-adhering contact paper used to cover the polystyrene walls. The covering proved remarkably durable and stable in radiation properties. After hundreds of experiments

performed during a period of more than a year, the heat transfer coefficients reproduced themselves within the 0.5–1% scatter of the data.

Thermal environment

The quality of experimentally determined, natural convection-related heat transfer results is highly sensitive to the thermal environment in which the experiments are performed. The laboratory used for the present experiments provided ideal conditions for natural convection work. It was thermally isolated by walls, a ceiling, and a floor backed by 45 cm of cork. There were no ducts or vents passing into or out of the laboratory. It was a room within a still larger room in a deep basement. Its relatively large volume (~ 70 m^3) contained numerous high heat capacity objects.

Power supplies and instrumentation were located in an adjacent room, so that the data acquisition could be accomplished without entering the laboratory.

Temperature stability during a typical 24-h period was about 0.03°C. Stratification only occurred at the high temperature runs ($T_w - T_\infty \sim 50$°C), but then it was only about 0.06°C per 30 cm elevation. The ambient temperature was measured at three elevations to the side of the cylinder by shielded thermocouples.

Experimental procedures

The initial experiments were performed in the absence of the walls shown in Figs. 1(a)–(c). These experiments included data runs for both the polished aluminum surface and the plastic-covered surface. The heat transfer results from these interaction-free experiments will serve as baseline information for correlating the effects of wall–cylinder interactions.

The experiments involving wall–cylinder interactions were carried through for Figs. 1(a)–(c) with the plastic-coated cylinder, after which verification runs for the no-walls case were made. Then, the coating was removed and the wall–cylinder interaction runs for the polished-surface case were performed.

Throughout the experiments, the wall–cylinder separation distances S_h and S_v [Figs. 1(a)–(c)] were varied by moving the walls while the cylinder remained fixed. For Fig. 1(c) it was found convenient to run through a succession of S_v values for each of several fixed values of S_h.

A minimum of 12 h was allowed for the attainment of steady state for each data run. This time was needed to accommodate the slow thermal response of the insulation walls.

Radiation properties

The primary radiation property measurements were made with a Gier–Dunkle heated-cavity reflectometer. The actual test cylinder could not be directly used in the radiation property measurement. Instead, flat aluminum specimens were prepared using the same polishing procedure as was used to polish the cylinder. The measured emissivity of the polished specimens was 0.050. The emissivity of the contact paper was measured both as a covering of polished aluminum and as a covering of polystyrene insulation. Within the slight scatter of repeated measurements, the results for the two cases were the same: $\varepsilon = 0.855$.

A secondary determination of the ε value of the contact paper was made by using the present experimental apparatus. For the no-walls case, natural convection heat transfer coefficients were determined by running experiments with the uncovered cylinder and subtracting the radiation contribution by using $\varepsilon = 0.05$ for the polished aluminum. Then, still without the walls, heat transfer measurements were made with the plastic-coated cylinder. With the aforementioned natural convection heat transfer coefficients as input information, it was found that the measured heat transfer rates for the covered cylinder could be best matched by computation if the ε value of the contact paper was 0.855. This independent determination of ε verifies the direct measurement.

PRESENTATION FORMAT AND DATA REDUCTION

The primary focus of this investigation was to identify the effects of wall–cylinder interactions and to provide information for calculating the cylinder heat transfer rate in the presence of such interactions. To these ends, the cylinder heat transfer results will be presented in terms of the ratio Q/Q^*. The quantity Q is the cylinder heat transfer rate in the presence of wall–cylinder interactions, while Q^* denotes the cylinder heat transfer rate in the absence of interactions. Both Q and Q^* correspond to the same cylinder surface radiation properties and to the same values of the cylinder temperature T_{cyl} and of the ambient temperature T_∞.

The departures of Q/Q^* from one provide an immediate measure of the effects of the interactions, with $Q/Q^* > 1$ indicating enhancement and $Q/Q^* < 1$ indicating degradation.

During the course of the present investigation, both Q and Q^* were measured, enabling the Q/Q^* ratio to be plotted as a function of the independent variables, as will be presented shortly. Note that aside from extraneous losses, Q and Q^* represent the rate of heat transfer from the cylinder via all of the participating transport mechanisms. The only extraneous loss that need be considered for the present experimental setup is conduction at the ends of the cylinder, and this loss was shown by calculation to be negligible. Thus, Q and Q^* were obtained directly from the measured electric power inputs.

The independent variables to be used in the presentation of the results will now be considered. During the course of the experiments, the separation distances, S_h and S_v and the cylinder–ambient temperature difference $(T_{cyl} - T_\infty)$ were varied, with each quantity being assigned either five or six values. The separation distances, expressed in dimensionless form as S_h/D and S_v/D, will be used to parameterize the

Q/Q^* values, while a dimensionless form of $(T_{cyl}-T_\infty)$ will be used as the abscissa variable. For the latter, the Rayleigh number

$$Ra = [g\beta(T_{cyl}-T_\infty)D^3/\nu^2]Pr \quad (1)$$

is suitable. The thermophysical properties appearing in Ra were evaluated at $\frac{1}{2}(T_{cyl}+T_\infty)$, except that $\beta = 1/T_\infty$ (absolute temperature).

Thus, in the presentation of results, Q/Q^* will be plotted vs Ra for parametric values of S_h/D and/or S_v/D and for specified values of the emissivities ε_{cyl} and ε_w. This format conveys the heat transfer results in a manner that is useful for applications.

In the application of the present results to find Q for a cylinder which experiences interactions with adjacent walls, the Q/Q^* ratio is read from the appropriate graph among those given here. Then, to calculate Q, information for Q^* is needed. Since there are no near-wall interactions for Q^* (i.e. no direct heat conduction from the cylinder to a wall)

$$Q^* = Q_{nc} + Q_{rad}. \quad (2)$$

In this expression, Q_{nc} represents the rate of heat transfer by natural convection from a cylinder situated in expansive surroundings, so that

$$Q_{nc} = hA(T_{cyl}-T_\infty) = \pi Lk(T_{cyl}-T_\infty)Nu \quad (3)$$

where Nu is the Nusselt number for natural convection about a horizontal cylinder, and the other quantities are defined in the Nomenclature.

The radiation component Q_{rad} in equation (2) corresponds to the case of a small body (i.e. the cylinder) in a large isothermal-walled enclosure. If it is assumed, as is common, that the ambient air temperature T_∞ and the enclosure wall temperature are equal, then

$$Q_{rad} = \varepsilon_{cyl}\sigma A(T_{cyl}^4 - T_\infty^4) \quad (4)$$

in which ε_{cyl} is the graybody emissivity of the cylinder surface. Equations (2)–(4) may be combined to give

$$Q^* = \pi Lk(T_{cyl}-T_\infty)Nu + \varepsilon_{cyl}\sigma\pi DL(T_{cyl}^4 - T_\infty^4). \quad (5)$$

Equation (5) can be used in applications to obtain Q^* values to complement the present graphical results for Q/Q^*. In this regard, comments about the natural convection Nusselt number that appears in equation (5) are in order.

From the present experiments performed without the presence of adjacent walls, all quantities in equation (5) were measured or were otherwise known aside from Nu, thereby enabling its determination. Within a data scatter of 1–2%, these Nusselt numbers were correlated via least squares as

$$Nu = 0.592Ra^{0.23} \quad (6)$$

over the range $2\times10^4 \leqslant Ra \leqslant 2\times10^5$. This result may be compared with the correlation due to Morgan [3], which is believed to be the most reliable available in the current literature. That correlation is

$$Nu = 0.480Ra^{1/4}. \quad (7)$$

Over the range of the present experiments, the maximum deviation between equations (6) and (7) is only 3.3%. This excellent level of agreement provides strong affirmation of the present experimental technique.

For use in equation (5), there is little to choose between equations (6) and (7). However, for consistency with the Q/Q^* results, equation (6) is recommended.

HEAT TRANSFER RESULTS

The primary focus in the presentation of the heat transfer results is the case where both the cylinder and the interacting wall(s) are surfaces of high emissivity. For this case, results will be presented for the three types of wall–cylinder interactions that are shown in Figs. 1(a)–(c).

The results for the configurations shown in Figs. 1(a) and (b) are given in Fig. 2. For each of these configurations, the cylinder interacts with a single wall. In the configuration shown in Fig. 1(a), there is a vertical wall situated to the side of the cylinder, but no bottom wall. Thus, for this configuration, the geometrical aspects of the wall–cylinder interaction are expressed by S_h/D. The configuration shown in Fig. 1(b) corresponds to a horizontal wall beneath the cylinder, but no side wall. Here, the geometric aspects are expressed by the S_v/D ratio. The Q/Q^* results for the configurations in Figs. 1(a) and (b) are plotted in the lower and upper graphs of Fig. 2, respectively.

Attention will first be turned to the results for the interaction between the cylinder and a side wall. As seen in Fig. 2 (lower diagram), S_h/D was assigned six values ranging from a closest spacing of 1/12 to a largest spacing of 4/3. These fractional values reflect the fact that the feeler gauges used to set S_h were made in 1/8 in. modules and that $D = 1.5$ in.

The main message of Fig. 2 is that the presence of a closely positioned side wall degrades the cylinder heat

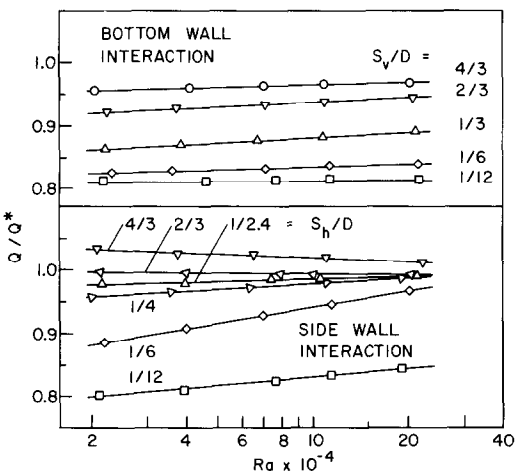

FIG. 2. Cylinder heat transfer in the presence of a side wall (lower graph) and a bottom wall (upper graph) for high emissivity cylinder and wall surfaces.

transfer relative to that when there is no wall. The degradation is, however, moderate. Thus, for the closest spacing used here ($S_h/D = 1/12$), the wall interaction reduces the heat transfer by 15–20% over the range of the investigated temperature differences (i.e. Rayleigh numbers). As the spacing increases, the extent of the degradation diminishes. For $S_h/D = \frac{1}{4}$, the reduction is only in the 2–4% range. Therefore, side wall–cylinder interactions can be neglected for $S_h/D \geqslant \frac{1}{4}$.

At the largest $S_h/D(=4/3)$, Q exceeds Q^* by 1–3%. This finding is believed to be real (i.e. not data scatter). It may be attributed to the supplementary buoyancy induced by the side wall, whose temperature is slightly elevated with respect to ambient as a result of its radiative interaction with the cylinder.

Another interesting observation about the figure in question is that Q/Q^* is relatively insensitive to the temperature difference (Rayleigh number). The typical variation in Q/Q^* is a few percent over the investigated order of magnitude range of Ra. This finding indicates that the ratio of Q and Q^* very nearly cancels the effect of the temperature difference. There is, however, no reason to expect that the residual variation of Q/Q^* with temperature difference is of the same order of magnitude and slope for all of the spacings.

The cylinder heat transfer results in the presence of bottom wall interactions will now be discussed. From the upper graph of Fig. 2, it is seen that for all the investigated spacings $1/12 \leqslant S_v/D \leqslant 4/3$, $Q/Q^* < 1$, indicating a degradation in the cylinder heat transfer. Once again, the degradation is moderate, with Q/Q^* lying in the range between 0.81 and 0.97. The smallest values of Q/Q^* correspond to the closest spacing, and Q/Q^* increases as the spacing grows larger. For $S_v/D = 4/3$, the reduction in heat transfer is 3–4%, so that bottom wall–cylinder interactions can be neglected when $S_v \geqslant 4/3$.

It is interesting to compare the cylinder heat transfer results for the bottom and side wall interactions. At the closest spacing ($S_h/D = 1/12$, $S_v/D = 1/12$), the Q/Q^* values for the two cases are nearly the same (0.81 vs 0.80–0.84). However, at larger spacings, the Q/Q^* for the bottom wall interaction are smaller than those for the side wall interaction, i.e. the presence of the bottom wall causes a somewhat greater reduction ($\sim 5\%$) in the cylinder heat transfer. It may also be seen that the Q/Q^* values for the bottom wall interaction are even less sensitive to temperature difference than those for the side wall interaction.

Attention will now be turned to the cylinder heat transfer results which correspond to interactions between the cylinder and a corner as portrayed by the configuration in Fig. 1(c). As seen there, it is necessary to specify both S_h and S_v in order to describe the geometrical aspects of the interaction.

The heat transfer results for the corner–cylinder interaction are presented in Figs. 3–5. These figures contain a total of six graphs. Each graph corresponds to a fixed separation distance between the cylinder and the vertical side wall, i.e. to a fixed value of S_h/D, and the successive graphs are arranged according to increasing values of S_h/D. For each side wall position, the vertical separation distance S_v/D between the cylinder and the bottom wall is varied parametrically from $S_v/D = 1/12$ to ∞ (bottom wall absent). In each graph, Q/Q^* is plotted as a function of the Rayleigh number.

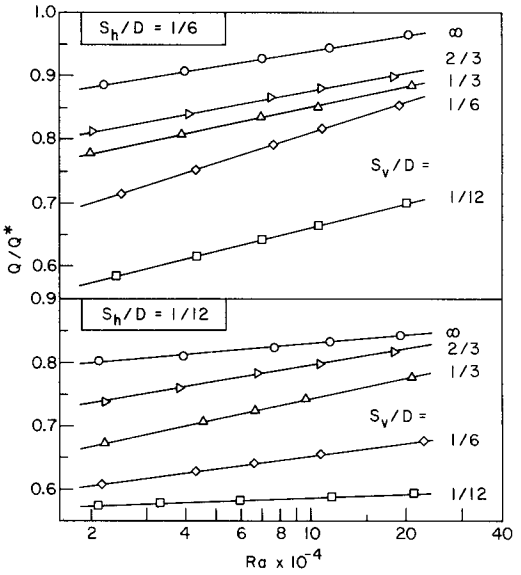

FIG. 3. Cylinder heat transfer in the presence of a corner for high emissivity cylinder and wall surfaces, $S_h/D = 1/12$ and 1/6.

In appraising Figs. 3–5, it is relevant to note that the uppermost set of data in each graph corresponds to the case where only the side wall is present. Thus, the bottom wall which forms one face of the corner is responsible for further reductions in the cylinder heat transfer that are additional to the reductions sustained

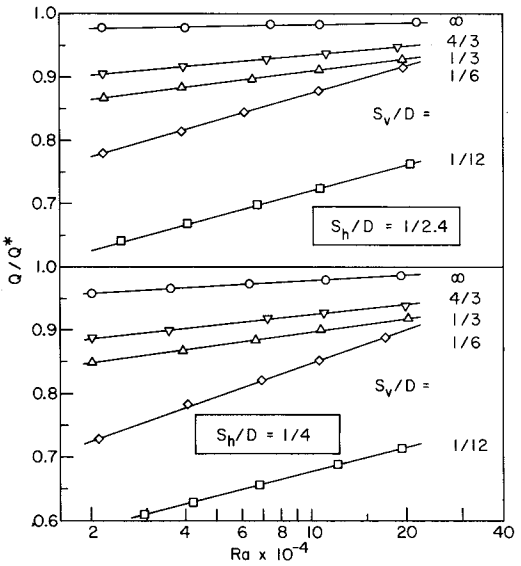

FIG. 4. Cylinder heat transfer in the presence of a corner for high emissivity cylinder and wall surfaces, $S_h/D = 1/4$ and 1/2.4.

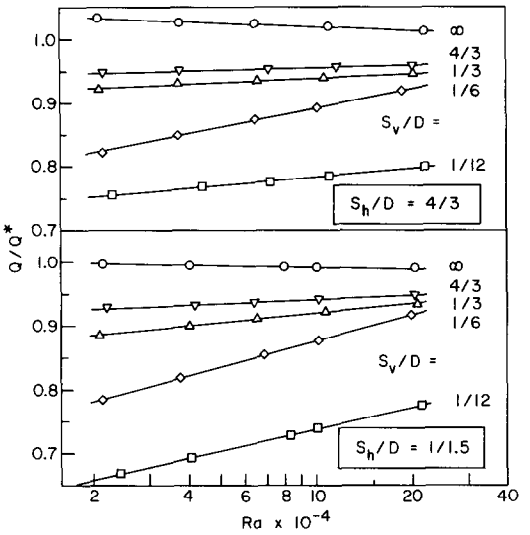

FIG. 5. Cylinder heat transfer in the presence of a corner for high emissivity cylinder and wall surfaces, $S_h/D = 1/1.5$ and 4/3.

for the side-wall-only case. These additional reductions can be appreciable. For example, if the S_v/D value for the bottom wall of the corner is 1/12 (the closest position of the bottom wall), the Q/Q^* values are 0.25–0.30 lower than those encountered when only the side wall is present.

The overall range of the Q/Q^* values in Figs. 3–5 is 0.57–1.03. The lower bound value, 0.57, corresponds to the closest spacings of both walls, $S_h/D = 1/12$ and $S_v/D = 1/12$. At the upper bound, $S_h/D = 4/3$ and $S_v/D = \infty$. For an intermediate case such as $S_h/D = \frac{1}{4}$ and $S_v/D = 1/3$, the heat transfer reductions are moderate, as reflected by Q/Q^* values ranging from 0.85 to 0.92. In general, if close spacings ($S_h/D \leqslant 1/6$ and $S_v/D \leqslant 1/6$) are excluded, the reductions in cylinder heat transfer due to interactions with the corner are no greater than 20%.

The Q/Q^* ratio responds to variations in S_h/D and S_v/D in a manner that is both regular and logical. At a fixed side wall spacing S_h/D, Q/Q^* is smallest at the closest bottom wall spacing and increases monotonically as S_v/D increases. With regard to the effect of S_h/D, a comparison of the successive graphs in Figs. 3–5 indicates an increasing level of Q/Q^* as S_h/D increases.

The fact that Q/Q^* increases monotonically with increasing S_h/D and S_v/D suggests that short-range direct conduction between the cylinder and the wall(s) did not play a decisive role in the experimental results. Had the direct conduction been significant, Q/Q^* would have displayed an increase with decreasing values of S_h/D and/or S_v/D in the range of small spacings. It is believed that the conduction effect was made minimal by the small cylinder–wall temperature differences which resulted from the radiative heating of the wall(s) by the cylinder.

As was noted in the Introduction, supplementary experiments were carried out in which the exposed surface of the cylinder was highly polished aluminum with an emissivity $\varepsilon_{cyl} = 0.05$. These experiments were performed more out of curiosity than in response to industrial applications. Consequently, only enough data were collected to establish broad trends.

The Q/Q^* results for the low emissivity (aluminum surface) cylinder are presented in Fig. 6. In this ratio, both Q and Q^* correspond to the low emissivity case. In particular, the Q^* in Fig. 6 is different from the Q^* in Figs. 2–5. The latter Q^* is for a cylinder having a high emissivity surface.

Figure 6 conveys the results for the cylinder heat transfer in the presence of corner–cylinder interactions, with the results corresponding to side-wall-only interactions included as a special case (i.e. $S_v/D = \infty$). The figure contains three graphs for fixed values of the side wall spacing $S_h/D = 1/12$, 1/6, and 1/3, respectively. In each graph, the bottom wall spacing S_v/D is varied from 1/12 to ∞.

The main message of Fig. 6 can be identified by comparisons with counterpart graphs among Figs. 2–5. Such comparisons show that Q/Q^* values for the low emissivity cylinder are consistently higher than those for the high emissivity cylinder. The differences in Q/Q^* for the two emissivity levels are about 0.15 for the corner–cylinder interaction and 0.05–0.10 for the side wall–cylinder interaction.

It follows from the foregoing that the degradation in cylinder heat transfer due to wall–cylinder interactions is greater when both natural convection and radiation play important roles than when natural convection is dominant. This finding discourages the application of information obtained for the latter situation to the former.

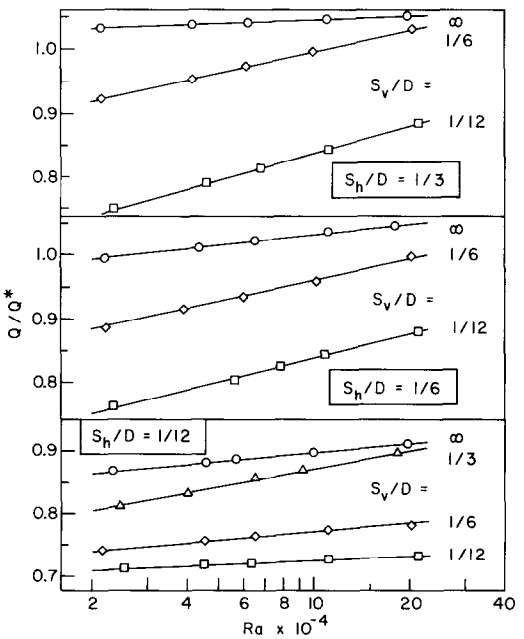

FIG. 6. Cylinder heat transfer in the presence of a corner for low emissivity cylinder surface and high emissivity wall surface(s).

WALL TEMPERATURE RESULTS

Representative wall temperature results will now be presented. As noted earlier, a thermocouple was installed at the surface of the side wall at the point of closest approach of the cylinder, as shown by the symbol TC in Figs. 1(a) and (c). This location was selected because the temperature at that point should be indicative of the highest value attained on the wall surface for a given configuration and given operating conditions. The measured wall temperatures T_w will be presented in terms of the dimensionless ratio $(T_w - T_\infty)/(T_{cyl} - T_\infty)$. This ratio, which compares the temperature rise of the wall above ambient with the temperature rise of the cylinder above ambient, is bounded between zero and one. The temperature data plotted in the forthcoming figures correspond to the high emissivity cylinder surface.

Figure 7 conveys wall temperature results for the case in which the cylinder interacts with a side wall without the presence of a bottom wall. In the figure, the dimensionless wall temperature is plotted as a function of the wall–cylinder separation distance S_h/D for two nominal values of the Rayleigh number, 2×10^4 and 2×10^5. As expected, the wall temperature is highest at the closest spacing and decreases as the spacing increases. Higher values are attained at lower Rayleigh numbers, which is consistent with the lower velocities (and mass flows) that prevail. At the closest spacing ($S_h/D = 1/12$) and lowest Rayleigh number, the wall temperature rise is almost 60% of the wall–ambient temperature difference. A residual temperature rise of about 10% prevails at the largest investigated spacing ($S_h/D = 4/3$).

Wall temperature results corresponding to corner–cylinder interactions are presented in Fig. 8. For each of three side wall spacings ($S_h/D = 1/12, 1/2.4$, and $4/3$), the dimensionless wall temperature is plotted vs the bottom wall spacing S_v/D over the range from 1/12 to 4/3, with the $S_v/D = \infty$ data indicated separately on the RHS of the figure. The figure shows that the wall temperatures attained in the presence of the corner are substantially higher than those which occur in the presence of a side wall alone. The highest wall temperature rise in evidence in Fig. 8 is 86% of the cylinder temperature rise above ambient. High wall temperatures prevail at all S_v/D for $S_h/D = 1/12$ and over a substantial range of S_v/D for $S_h/D = 1/2.4$.

The elevated wall temperatures affect the cylinder heat transfer in several ways. The occurrence of such temperatures diminishes both the radiative transfer and the direct short-range conduction. On the other hand, an additional upward buoyancy is induced because $T_w > T_\infty$. The magnitudes of the separate effects cannot be determined from the available data.

CONCLUDING REMARKS

The research reported here has been concerned with the all-modes heat transfer from a horizontal cylinder in the presence of adjacent adiabatic walls which partially enclose the fluid space in which the cylinder is situated. Three types of wall systems were used, including a vertical wall situated to the side of the cylinder, a horizontal wall beneath the cylinder, and a corner formed by the intersection of the vertical and horizontal walls. The separation distance between the cylinder and the wall(s) was varied parametrically, with the closest spacing between the cylinder periphery and the wall being 1/12 cylinder diameter. In the main set of data runs, the surfaces of the cylinder and the wall(s) were of high emissivity. Supplementary runs were made with a low emissivity cylinder surface. The wall–ambient temperature difference was varied by an order of magnitude. All the experiments were performed in air.

In general, the wall–cylinder interactions tended to reduce the cylinder heat transfer relative to that for a non-interacting cylinder. Closer spacing resulted in reduced heat transfer. For the case of side wall interactions (no bottom wall), the largest heat transfer

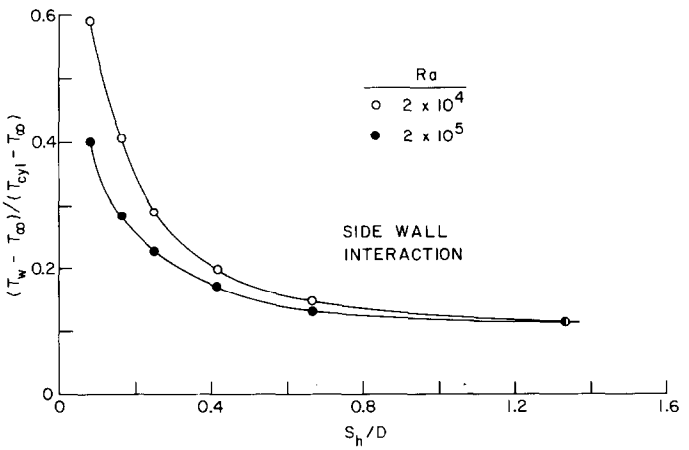

FIG. 7. Temperature on side wall at point of closest approach to the cylinder, side wall–cylinder interactions; high emissivity cylinder and wall surfaces.

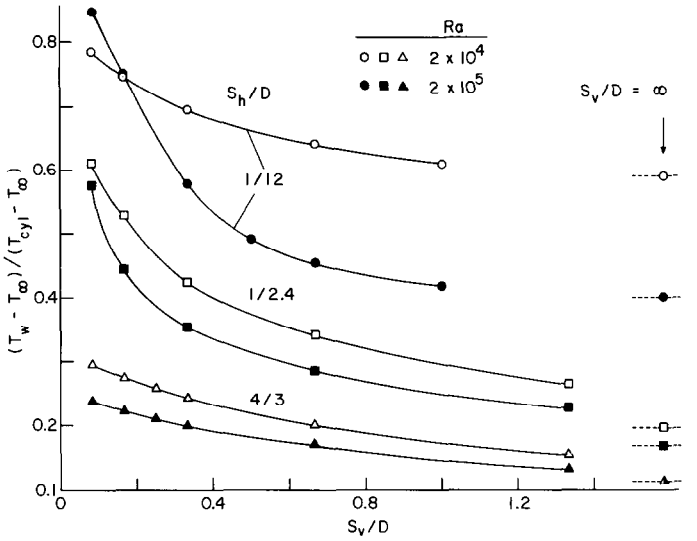

FIG. 8. Temperature on side wall at point of closest approach to the cylinder; corner–cylinder interactions; high emissivity cylinder and wall surfaces.

reduction was about 20%. The reductions were negligible when the spacing between the cylinder periphery and the wall was 1/4 cylinder diameter or greater. In the presence of a bottom wall (without a side wall), the heat transfer reductions were greater by about 5% than those caused by a side wall. A spacing of $1\frac{1}{3}$ cylinder diameters or greater was required to eliminate the effects of the bottom wall interactions.

The effect of a corner was found to be substantially greater than the effects of either a side wall or a bottom wall. At the closest investigated spacing, the corner-induced heat transfer reduction was about 40%. The reductions were limited to 20% for spacings of 1/4 diameter and greater.

The aforementioned specifics pertain to the case of the high emissivity cylinder surface, although the trends also hold for the low emissivity cylinder surface. The experiments using the low emissivity surface showed that the reduction in cylinder heat transfer due to wall–cylinder interactions is greater when both natural convection and radiation play important roles than when natural convection is dominant.

The heat transfer results are presented in ratio form. The numerical values of the heat transfer ratio should be applicable not only for the specific cylinder emissivities of the experiments but also for emissivities which deviate moderately from these values.

There was no indication in the heat transfer results that short-range, direct heat conduction between the cylinder and the wall(s) played a major role.

Measurements showed that the adiabatic wall(s) could attain relatively high temperatures due to interactions with the cylinder. The maximum wall temperature rise relative to ambient, which occurred in the presence of corner–cylinder interactions and at the closest cylinder spacing, was 86% of the cylinder–ambient temperature difference.

REFERENCES

1. C. D. Jones and D. J. Masson, An interferometric study of free convection heat transfer from enclosed isothermal surfaces, *Trans. Am. Soc. Mech. Engrs* **77**, 1275–1281 (1955).
2. L. M. K. Boelter and V. H. Cherry, Measurement of heat transfer by free convection from cylindrical bodies by the Schlieren method, *Trans. Am. Soc. Heat Vent. Engrs* **44**, 499–512 (1938).
3. V. T. Morgan, The overall convective heat transfer from smooth circular cylinders, in *Advances in Heat Transfer*, Vol. 11, pp. 199–264. Academic Press, New York (1975).

DIFFERENTS MODES DE TRANSFERT THERMIQUE POUR UN CYLINDRE HORIZONTAL ADJACENT A DES PAROIS ADIABATIQUES ET PARTIELLEMENT LIMITANTES

Résumé—Le transfert thermique relatif aux différents modes est mesuré pour un cylindre horizontal chauffé, en présence de parois adiabatiques qui ferment partiellement l'espace dans lequel le cylindre est situé. Les trois configurations étudiées concernent une paroi verticale située contre le cylindre, une paroi horizontale sous le cylindre, et un coin formé par des parois verticale et horizontale. La distance entre cylindre et paroi(s) est variable, avec le plus petit espacement entre périphérie du cylindre et paroi(s) égal à 1/12 du diamètre du cylindre. Dans la plupart des expériences, les surfaces du cylindre et des parois sont à forte émissivité. En général les interactions paroi-cylindre réduisent le transfert thermique du cylindre, avec de plus grandes réductions pour les plus petits espacements. En présence de la paroi latérale, la plus forte réduction mesurée est d'environ 20%; pour des espacements de 1/4 du diamètre et plus, les réductions sont négligeables. La paroi basse (sans paroi latérale) cause des réductions plus fortes de 5% que celles dues à la paroi latérale, tandis que le coin apporte des réductions nettement plus grandes (jusqu'à 40%). Des expériences supplémentaires avec un cylindre de faible émissivité montrent que les effets du rayonnement jouent un rôle sensible dans les réductions du transfert thermique du cylindre.

GESAMTWÄRMEÜBERGANG AN EINEM HORIZONTALEN ZYLINDER IN DER NÄHE VON IHN TEILWEISE UMSCHLIESSENDEN ADIABATEN WÄNDEN

Zusammenfassung—Es wurde der Gesamtwärmeübergang eines horizontalen, beheizten Zylinders gemessen, der an adiabate Wände grenzt und von diesen teilweise umschlossen ist. Drei Fälle wurden untersucht: eine vertikale Wand an der Stirnseite des Zylinders, eine horizontale Wand unter dem Zylinder und eine Ecke, die durch den Schnittpunkt der horizontalen und der vertikalen Wand gebildet wurde. Die Entfernung zwischen dem Zylinder und der Wand (den Wänden) diente als Parameter für den Gesamtwärmeübergang. Der kleinste Abstand zwischen dem Zylinderrand und der Wand (den Wänden) betrug 1/12 Zylinderdurchmesser. Bei den meisten Experimenten hatte die Oberfläche des Zylinders und der Wand (der Wände) einen hohen Emissionskoeffizienten. Im allgemeinen wird der Wärmeübergang des Zylinders durch die Wechselwirkung von Zylinder und Wand reduziert mit einer größeren Abnahme bei kleineren Zwischenräumen. Bei der vertikalen Wand betrug die größte gemessene Abnahme 20%; bei Zwischenräumen von 1/4 Zylinderdurchmesser und größer ist die Abnahme vernachlässigbar. Eine horizontale Wand unter dem Zylinder (ohne Seitenwand) brachte eine um 5% größere Abnahme als die Seitenwand, während die Wechselwirkung zwischen der Ecke und dem Zylinder eine wesentlich höhere Verringerung brachte (40%). Ergänzende Experimente an einem Zylinder mit geringerem Emissionskoeffizienten zeigten, daß die Strahlungseinflüsse eine wesentliche Rolle bei der Abnahme des Wärmeübergangs durch Wandeinflüsse spielen.

ТЕПЛОПЕРЕНОС ОТ ГОРИЗОНТАЛЬНОГО ЦИЛИНДРА, РАСПОЛОЖЕННОГО ВБЛИЗИ АДИАБАТИЧЕСКИХ, ЧАСТИЧНО ЗАКРЫВАЮЩИХ ЕГО СТЕНОК

Аннотация—Проведено измерение интенсивности теплообмена, осуществляемого всеми видами теплопереноса, нагреваемого горизонтального цилиндра вблизи адиабатических стенок, частично закрывающих пространство, в котором расположен цилиндр. Исследовались три конфигурации: цилиндр с расположенной сбоку от него вертикальной стенкой, цилиндр с расположенной под ним горизонтальной стенкой и цилиндр в углу, образованном вертикальной и горизонтальной стенками. Расстояние между цилиндром и стенками изменялось параметрически, причем наименьшее расстояние равнялось 1/12 диаметра цилиндра. В большей части экспериментов поверхности цилиндра и стенок имели большую излучательную способность. Как правило, в результате взаимодействия стенок с цилиндром теплоперенос от цилиндра снижался, причем тем сильнее, чем меньше было расстояние между ними. Когда стенка находилась сбоку от цилиндра, максимальное снижение достигало 20%; при расстояниях, равных 1/4 диаметра цилиндра и более, снижение теплоотдачи было пренебрежимо малым. Когда цилиндр помещался над горизонтальной стенкой (без боковой), теплоотдача снижалась примерно на 5% больше, чем в первом случае, а когда присутствовала еще и боковая стенка, это снижение было значительным и достигало 40%. Дополнительные эксперименты, проведенные на цилиндре с низкой излучательной способностью, показали, что излучение играет большую роль в процессе снижения теплоотдачи цилиндра при взаимодействии со стенками.